Air-Gap Convection in Rotating Electrical Machines

David A. Howey, *Member, IEEE*, Peter R. N. Childs, and Andrew S. Holmes, *Member, IEEE*

***Abstract*—This paper reviews the convective heat transfer within the air gap of both cylindrical and disk geometry rotating electrical machines, including worked examples relevant to fractional horsepower electrical machines. Thermal analysis of electrical machines is important because torque density is limited by maximum temperature. Knowledge of surface convective heat transfer coefficients is necessary for accurate thermal modeling, for example, using lumped parameter models. There exists a wide body of relevant literature, but much of it has traditionally been in other application areas, dominated by mechanical engineers, such as gas turbine design. Particular attention is therefore given to the explanation of the relevant nondimensional parameters and to the presentation of measured convective heat transfer correlations for a wide variety of situations from laminar to turbulent flow at small and large gap sizes for both radial-flux and axial-flux electrical machines.**

***Index Terms*—Convection, electrical machine, heat transfer, thermal analysis.**

I. Introduction

THE electromagnetic analysis of motors and generators is a mature subject; in contrast, the thermal and aerodynamic aspects of electrical machine design have been less thoroughly researched to date [1]. Modern machines must be compact, light, and torque dense and are often required to withstand extreme environmental and loading conditions. Knowledge of the airflow in a machine is crucial for design purposes, particularly where air-gap convection limits heat transfer. The surface convective heat transfer coefficients, important for the calculation of temperatures, are complex functions of geometry and fluid mechanics. This paper seeks to give an overview of the state of the art in airflow and convection within the air gap in cylindrical- and disk-type machines, with a particular emphasis on experimentally measured convection data in the form of correlations that can be applied during the design. It also seeks to summarize the typical flow patterns that might arise, some of which are quite counterintuitive. Other related thermal topics, such as lumped parameter (LP) modeling, radiation heat transfer, thermal contact resistances, and finite-element analysis, are not discussed in detail since they have been covered elsewhere, e.g., in [2] and [3].

Manuscript received May 31, 2010; revised September 18, 2010; accepted November 29, 2010. Date of publication December 17, 2010; date of current version October 25, 2011.

D. A. Howey and P. R. N. Childs are with the Department of Mechanical Engineering, Imperial College London, SW7 2AZ London, U.K. (e-mail: d.howey@imperial.ac.uk).

A. S. Holmes is with the Department of Electrical and Electronic Engineering, Imperial College London, SW7 2AZ London, U.K.

Color versions of one or more of the figures in this paper are available online at http://ieeexplore.ieee.org.

Digital Object Identifier 10.1109/TIE.2010.2100337

In an electrical machine, the internal temperatures reached at a given operating point must be predicted during design because of the following reasons.

1) The calculation of the maximum continuous rating requires an adequate thermal model to ensure that the cooling provision is sufficient to avoid overheating since the torque density (and therefore the maximum rms current density in the windings) is thermally limited in a machine of good electromagnetic design.
2) The stator temperature affects the efficiency because the resistivity of the copper windings increases with temperature. For example, at 100 °C, the resistivity of copper is increased by almost 30% compared to room temperature.
3) Materials such as permanent magnets (PMs) and polymers used in stator construction can only typically withstand continuous maximum temperatures of about 150 °C.
4) Inaccurate predictions lead to the use of excessive safety margins. Improvements would reduce the number of prototype iterations required and minimize the cost. This is becoming increasingly important even in smaller machines.

Temperatures that are consistently too high will reduce the lifetime of the machine and may lead to serious failure. The main failure mechanism is the breakdown of the insulation surrounding the copper windings due to oxidation and embrittlement. This leads to a loss of mechanical strength and, eventually, breakage which may cause short circuits [4]. Although electrical machines may usually be overloaded for short periods of time, if the temperature exceeds the maximum acceptable temperature for the insulation class, then the lifetime will be shortened, perhaps severely.

A second failure mechanism in PM machines is the demagnetization of the magnets. The most commonly used PM material is neodymium–iron–boron (NdFeB). The demagnetization curve of NdFeB depends strongly on temperature [5]: As the magnet temperature increases, the material's crystal structure changes, and the magnitudes of B_r and H_c decrease. Additionally, the "knee" in the demagnetization curve moves up; if the magnets are operated below the knee, irreversible change takes place, making it important to ensure that the magnet temperatures remain modest at all times.

Internal heating in electrical machines is the result of losses. The temperature reached is governed by the balance between the heat generated, the heat removed, and the thermal capacity. Major sources of loss are Joule (I^2R) losses in the windings, core losses due to eddy currents and hysteresis, and mechanical

TABLE I
DEPENDENCE OF POWER LOSSES ON MACHINE AND OPERATING PARAMETERS [6], [7]

Joule loss	$\alpha\ I^2 R_{stator}$
Eddy current loss	$\alpha\ \Omega^2 B^2$
Hysteresis loss	$\alpha\ \Omega B^n$
Bearing loss	$\alpha\ \Omega m$
Windage loss	$\alpha\ \Omega^3 D^5 \rho$ (disc machine, $D >> L$)
	$\alpha\ \Omega^3 D^4 L \rho$ (drum machine, $L >> D$)

losses. Table I shows approximately how these depend on various operating parameters in an electrical machine: I is the stator current, R is the stator resistance, Ω is the shaft speed, m is the machine mass, D is the rotor diameter, L is the rotor axial length, B is the average magnetic flux density, and ρ is the air-gap fluid density.

A number of factors determine the rate of heat removal in an air-cooled electrical machine. The geometry and materials, surface areas, and machine size have an impact. Since the losses are roughly proportional to volume L^3 (where L is a length dimension), the surface area is proportional to L^2, and cooling may be more of a challenge in larger machines. Additionally, if a machine is totally enclosed, air will recirculate internally, and the heat transfer is typically limited by internal heat transfer (for example, conduction through insulating materials) and convection around the outside surfaces. However, the heat removal rate may be substantially increased if the machine can be throughflow ventilated, i.e., air continually enters from ambient, passes through, and is then expelled.

An aspect of thermal modeling not discussed in detail in this paper is the solid-domain thermal modeling. Heat transfer in the solid domain (e.g., in iron, copper, polymers, etc.) is by thermal conduction, governed by the heat equation

$$\frac{\partial T}{\partial t} = \alpha \nabla^2 T \tag{1}$$

where T is the temperature field, t is the time, and α is the thermal diffusivity of the material. This equation can be solved analytically by integration in 1-D cases and by Fourier series expansion in 2-D cases. For complex 2-D and 3-D geometries with many different material types and complicated boundary conditions, LP methods and numerical methods are usually applied. LP thermal network models are a common way to evaluate the thermal performance of electrical machines. The method assumes that the spatial distribution of temperature within each different material or subcomponent is uniform. Where this is not the case, subcomponents can be further broken down into smaller sections to increase the spatial resolution of the model; this is typically done, for example, within stator windings. The LP method is fast to compute and therefore can handle transient calculations with complex load cycles. It has been widely applied; for example, Mellor *et al.* [8] developed LP models for totally enclosed fan-cooled induction machines, and transient results are compared to experiments and are shown to be quite accurate. LP methods can equally be applied to disk-type machines; for example, Spooner and Chalmers [9] developed an LP model for an axial-flux permanent-magnet (AFPM) machine and obtained thermal conduction and contact resistances by conducting tests on a dummy rotor. LP models must be carefully "tuned" with empirical data, such as convective heat transfer correlations, to ensure adequate performance.

In summary, air-gap convection is crucial in the thermal modeling of electrical machines in order to achieve accurate results. In certain situations, the air-gap convection is the limiting factor for heat transfer, for example, in a throughflow-ventilated disk machine where all heat is removed by air passing over the stator surface or in a cylindrical induction machine where there may be significant heating within the rotor.

II. PREVIOUS REVIEWS

There are relatively few review papers on the subject of airflow and convection in rotating electrical machines. Boglietti *et al.* [2] reviewed the thermal analysis of electrical machines with a particular focus on LP models. Staton *et al.* [3] also reviewed the more challenging areas in thermal analysis, which include contact resistances, stator winding conductivity, and convection coefficients, particularly around end windings where there are complex flow paths. Staton and Cavagnino [10] reviewed convection in electrical machines, focusing on correlations for natural convection around the external casings of cylindrical geometry machines and also on correlatons for forced cooling with fans or water jackets. They included a small section on air-gap heat transfer. Disk-type machine geometries were not considered.

A recent overview of the flow in rotating components is given in a report from the Engineering Sciences Data Unit [7]; this addresses disks, cylinders, and cavities. Many correlations are given for the calculation of aerodynamic drag in different situations, but the scope of the report does not include heat transfer.

Childs and Long [11] reviewed experimental, numerical, and analytical investigations into forced convection heat transfer in annular passages. This is relevant, particularly in the design of cylindrical-type electrical machines.

III. NONDIMENSIONAL GROUPS

Convection heat transfer data are normally nondimensionalized so that the number of variables in the problem is reduced, and results can be applied generally to a variety of machine sizes.

The most relevant nondimensional groups here are the Reynolds number Re, which encapsulates the rotor speed and machine size; the average Nusselt number Nu which is the nondimensional surface convective heat transfer coefficient; C_w which is the nondimensional air mass flow rate through a machine; and geometric parameters such as the gap ratio G.

The Reynolds number and Nusselt number can be expressed using different characteristic lengths, e.g., the rotational Reynolds number Re_θ and Nusselt number Nu using the rotor radius or the gap Reynolds number Re_g and gap Nusselt number Nu_g using the gap size. For cylindrical annuli, the

Nusselt number is expressed in terms of the hydraulic diameter $D_h = 2g$. These various groups are defined as follows:

$$Re_g = \frac{\Omega g R}{\nu} \tag{2}$$

$$Re_\theta = \frac{\Omega R^2}{\nu} \tag{3}$$

$$Nu = \frac{hR}{k} \quad \text{for disk machines} \tag{4}$$

$$Nu = \frac{hD_h}{k} \quad \text{for cylindrical machines} \tag{5}$$

$$G = \frac{g}{R} \tag{6}$$

$$C_w = \frac{\dot{m}}{\mu R} \tag{7}$$

where R is the rotor radius, Ω is the speed, ν is the fluid kinematic viscosity (usually at ambient temperature), h is the convective heat transfer coefficient, k is the fluid conductivity (usually at ambient temperature), L is the length of a cylindrical machine, g is the gap size between the rotor and the stator, $\dot{m}$ is the air mass flow rate, and μ is the dynamic viscosity. There is another nondimensional group relevant in cylindrical geometry machines, the Taylor number, which provides an indication of the relative effects of inertial forces and viscosity for an annulus with rotation of one or more of the cylindrical surfaces. The Taylor number based on mean annulus radius $r_m = (a+b)/2$ is defined as

$$Ta_m = \frac{\Omega_a r_m^{0.5} b - a^{1.5}}{\nu} \tag{8}$$

where a and b are the inner and outer annulus diameters, respectively.

A. Application of Thermal Modeling to Electrical Machines

There are various ways in which convective heat transfer coefficients can be applied. The usual approach, for example, in LP models is to obtain a convective heat transfer "thermal resistance." First, the appropriate Nusselt number correlation is selected for the situation, for example, $Nu = ARe_\theta^B$. The Nusselt number is calculated from the correlation, and then, the convective heat transfer coefficient h is calculated from (4) or (5). The convection thermal resistance is then given by

$$R = \frac{1}{hA} \tag{9}$$

where A is the area over which the heat transfer occurs. In a cylindrical machine, A is the stator or rotor surface bordering the air-gap annulus. In a disk machine, it is the circular stator or rotor surface bordering the air-gap space which is also disk shaped. Note that R is typically *not* constant (as commonly assumed in LP models) but varies as a function of machine geometry and rotor speed.

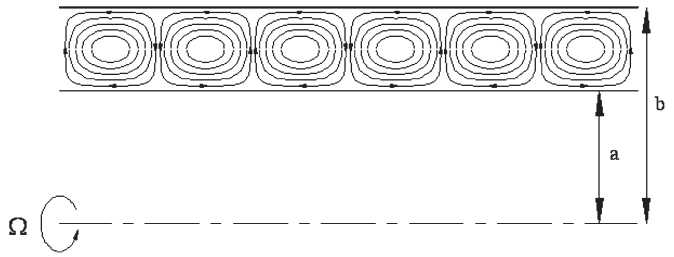

Fig. 1. Taylor vortices in an annulus with rotation.

IV. Cylindrical Geometry Machines

Cylindrical (or "drum") geometry electrical machines are the most common type of electrical machine. The air gap is an annulus formed between two concentric cylinders. The air-gap magnetic field lines are oriented in the radial direction, so these are also called radial-flux machines. There are many different machine types, e.g., induction machines, PM brushless machines, and switched reluctance machines. Flow and heat transfer in this geometry is also important to a wide number of other applications from shafts and axles to spinning projectiles to gas turbine engines.

A. Airflow in the Rotor–Stator Gap

Couette flow is the term used to describe the flow between two surfaces that are in close proximity such that the flow is dominated by viscous effects and inertial effects which are negligible. In cylindrical coordinates, this involves the flow in an annulus, and the Navier–Stokes equations can be solved exactly by analytical techniques, subject to a number of significant assumptions. The Couette flow in an annulus with rotation characterizes a system in which dynamic equilibrium exists between the radial forces and the radial pressure gradient. However, when it is not possible for the radial pressure gradient and the viscous forces to dampen out and restore the changes in the centrifugal forces caused by small disturbances in the flow, the fluid motion is unstable and results in a secondary flow. A simple criterion for determining the onset of instability was developed by Rayleigh [12]. In essence, the criterion determines whether the force due to inward radial pressure is adequate to maintain inward centripetal acceleration for an arbitrary element of fluid.

In real flows, the onset of this instability is modified by the action of viscosity and rotation of annular surfaces which can lead to instabilities in the flow with the formation of complex toroidal vortices, known for certain flow conditions as the Taylor vortices. The Taylor vortex flow represents a significant modeling challenge and has been subject to a vast number of studies. Experiments, e.g., by Taylor [13], revealed that the simple axisymmetric laminar flow in an annulus with a combination of inner and outer cylinder rotation was replaced by a more complicated eddying flow structure. If the angular velocity exceeded a critical value, a steady axisymmetric secondary flow in the form of regularly spaced vortices in the axial direction was generated as illustrated in Fig. 1. Alternate vortices rotate in opposite directions.

Taylor [13] formulated the stability problem, taking into account the effects of viscosity by assuming an axisymmetric

infinitesimal disturbance and solving the dynamic conditions under which instability occurs. Assuming that the annular gap size $g = b - a$ is small compared to the mean radius r_m, known as the small gap approximation, Taylor's solution for the angular velocity at which the laminar flow breaks down and the flow instabilities grow leading to the formation of secondary flow vortices, called the critical speed, is given by

$$\Omega_{cr} = \pi^2 \nu \sqrt{\frac{a+b}{2S\,(b-a)^3\, a^2\,[1-(\Omega_b/\Omega_a)\, b^2/a^2]\,(1-\Omega_b/\Omega_a)}} \tag{10}$$

where

$$S = 0.0571\left[\frac{1+\Omega_b/\Omega_a}{1-\Omega_b/\Omega_a} + 0.652\left(1-\frac{1}{x}\right)\right] + 0.00056\left[\frac{1+\Omega_b/\Omega_a}{1-\Omega_b/\Omega_a} + 0.652\left(1-\frac{1}{x}\right)\right]^{-1} \tag{11}$$

where $x = a/b$.

For the case of a stationary outer cylinder, $\Omega_b/\Omega_a = 0$, and therefore, (10) and (11) reduce to

$$\Omega_{cr} = \pi^2 \nu \sqrt{\frac{a+b}{2S\,(b-a)^3\, a^2}} \tag{12}$$

$$S = 0.0571\,[1 - 0.652\,(b-a)/a] + 0.00056\,[1 - 0.652\,(b-a)/a]^{-1}. \tag{13}$$

For the case of a narrow gap and stationary outer cylinder, $x \to 1$, so $\Omega_a/\Omega_b = 0$, and (10) and (11) give a critical speed which results in a critical Taylor number

$$Ta_{m,cr} = \sqrt{1697} = 41.19. \tag{14}$$

If the Taylor number exceeds this critical Taylor number, then Taylor vortices can form, whereas if $Ta_m < Ta_{m,cr}$, then the flow remains a Couette flow.

The critical angular velocity for this case is

$$\Omega_{cr} = \frac{41.19\nu}{r_m^{0.5}\,(b-a)^{1.5}}. \tag{15}$$

Fig. 2 shows the variation in Taylor number with rotor size and speed for the specific case of a machine with a narrow gap size of 0.5 mm. The air viscosity was $\nu = 18.9$e–6 m^2/s, assuming an air temperature of about 60 °C. It can be seen that, at higher speeds and larger rotor radii, there may be Taylor vortices in the gap since the Taylor number is greater than the critical Taylor number, also shown in the graph.

For an annulus with a larger size finite gap

$$\Omega_{cr} = \frac{41.19\nu F_g}{r_m^{0.5}\,(b-a)^{1.5}} \tag{16}$$

where F_g is a geometrical factor defined by

$$F_g = \frac{\pi^2}{41.19\sqrt{S}}\left(1-\frac{b-a}{2r_m}\right)^{-1} \tag{17}$$

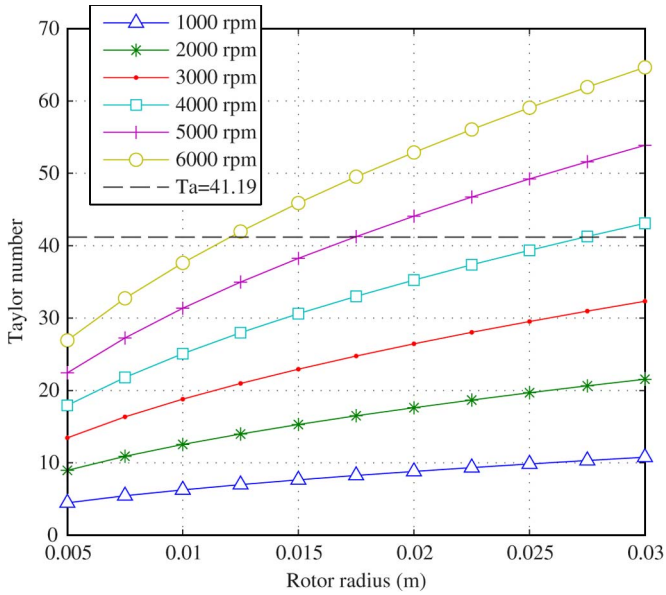

Fig. 2. Taylor number versus rotor size and speed for 0.5-mm gap machine.

and S is given in an alternative form by

$$S = 0.0571\left(1 - 0.652\frac{(b-a)/r_m}{1-(b-a)/2r_m}\right) + 0.00056\left(1 - 0.652\frac{(b-a)/r_m}{1-(b-a)/2r_m}\right)^{-1}. \tag{18}$$

The wavelength for the instability is approximately $\lambda = 2(b-a)$.

B. Convective Heat Transfer

At low Taylor numbers, the flow is a laminar shear flow, and for $Ta_m^2/F_g^2 < 1700$, the heat transfer is dominated by conduction and can be predicted for the inner or outer surface using the correlation developed by Bjorklund and Kays [14]

$$Nu = \frac{hD_h}{k} = \frac{2\,[(b-a)/a]}{\ln\,[1+(b-a)/a]} \tag{19}$$

where, for the case of an annulus, $D_h = 2(b-a)$. For the machine geometry and speeds shown in Fig. 2, this correlation would be applied when $Ta < 41.19$, and since the heat transfer in (19) is independent of speed and is only a weak function of the radius in this range, inserting values gives $h \approx 58$ W/m$^2 \cdot$ K for 5 mm $\leq a \leq$ 30 mm.

For the laminar flow with vortices $(1700 < Ta_m^2/F_g^2 < 10^4)$, from Becker and Kaye [15], [16]

$$Nu = 0.128\left(Ta^2/F_g^2\right)^{0.367}. \tag{20}$$

For the machine geometry and speeds shown in Fig. 2, this correlation would be applied when $Ta > 41.19$.

For turbulent flow $(10^4 < Ta_m^2/F_g^2 < 10^7)$, from Becker and Kaye [15], [16]

$$Nu = 0.409\left(Ta^2/F_g^2\right)^{0.241}. \tag{21}$$

In (20) and (21), an annulus area based on the logarithmic mean radii $[(b-a)/ln(a/b)]$ has been used to evaluate the overall heat transfer.

The preceding correlations all apply to the totally enclosed case with no superposed axial throughflow, whereas the remainder of this section concerns the case of axial throughflow. Experiments using hot wire anemometry and flow visualization by Kaye and Elgar [17] revealed the existence of four modes of flow in this situation. Their tests were performed using an annulus with inner and outer radii of 34.9 and 47.5 mm, respectively, at axial throughflow Reynolds numbers of up to 2000 and rotational Reynolds numbers of up to 3000. The four regimes of flow corresponded to the following:

1) purely laminar flow;
2) laminar flow with Taylor vortices;
3) turbulent flow with vortices;
4) turbulent flow.

For the laminar flow with vortices, Simmers and Coney [18] used principles similar to the Reynolds analogy, which makes use of the fact that a similarity exists between the energy equation and momentum equation for heat transfer between the outer annulus surface and throughflow, giving

$$Nu = \frac{4\,\mathrm{Pr}\,Re_z^{0.5}\left(\Omega_a^2 ab^3/\nu^2\right)^{0.3675}}{B\left(A/\left(1-x\right)\right)^{0.5}\left(x/\left(1-x\right)\right)^{0.25}\left(\Omega_a^2 ab^3/\nu^2\right)_{cr}^{0.6175}} \tag{22}$$

where

$$A = \left[1+x^2+\left(\frac{1-x^2}{\ln x}\right)\right]\left(2+\frac{1-x^2}{\ln x}\right)^{-1} \tag{23}$$

$$B = \mathrm{Pr}+\ln\left\{1+\mathrm{Pr}\,\exp\left[\frac{2}{3}\left(\frac{1-x}{x}\right)^{0.25}\left(\frac{xA}{(1-x)^2}\right)^{0.5} Re_z^{-0.5}\left(\frac{\Omega_a^2 ab^3}{\nu^2}\right)^{0.1325}\left(\frac{\Omega_a^2 ab^3}{\nu^2}\right)_{cr}^{0.1175}-1\right]-Pr\right\} \tag{24}$$

$$Re_z = u_z D_h \nu, \text{ where } u_z \text{ is axial velocity.} \tag{25}$$

The Prandtl number Pr is the ratio of viscous to thermal diffusion rates, defined as

$$Pr = \frac{\mu c_p}{k}. \tag{26}$$

This is a fluid property. For gases, typically $Pr \approx 0.7$.

For the turbulent flow with vortices, Gazley [19] gave the following correlation based on tests at axial and rotational Reynolds numbers of up to 1.2e4 and 1.1e5, respectively

$$Nu = 0.03 Re_e^{0.8} \tag{27}$$

where the Reynolds number was based on the vector sum of the bulk axial flow and the rotor speed

$$Re_e = \frac{\sqrt{u_z^2+u_\phi^2}D_h}{\nu}. \tag{28}$$

Gazley looked at the effect of slotted features in the annulus, such as may be due to salient poles in an electrical machine, showing a corresponding small increase in heat transfer over the smooth surface condition.

Moreover, for the turbulent flow with vortices, Kosterin and Finatev [20] present the following correlation:

$$Nu = 0.018\left\{Re_z\left[1+0.6\left(\left(\Omega_a a D_h/\nu\right)/Re_z\right)^2\right]^{0.5}\right\}^{0.8} \tag{29}$$

for $0 < (\Omega_a a D_h/\nu) < 1\text{e}5$ and $3\text{e}3 < Re_z < 3\text{e}4$.

For turbulent flow in an annulus with inner cylinder rotation, Kuzay and Scott [21] present the following correlation based on measurements from a rig with a radius ratio of 0.57 for axial Reynolds numbers of up to 6.5e5 and rotational Reynolds numbers of up to 4e4:

$$Nu = 0.022\left[1+\left(\frac{D_h u_\phi}{\pi a u_z}\right)^2\right]^{0.8714} Re_z^{0.8} Pr^{0.5}. \tag{30}$$

Childs *et al.* [22] and Childs and Turner [23] present the following correlation based on experimental data for a large rotating drum of 400-mm diameter for turbulent flow heat transfer in an annulus with a stationary outer cylinder:

$$\frac{Nu - Nu_x}{Nu_x} = 0.068\left(\frac{u_\phi}{u_z}\right)^2 \tag{31}$$

where $Nu_x = 0.023 Re_z^{0.8}\sqrt{Pr}$ for $1.7\text{e}5 < Re_z =< 3.7\text{e}5$, $1.4\text{e}4 < Re_\phi = (\Omega a^2/\nu) < 2.7\text{e}6$, and $1.65 < z/D_h < 5$.

C. Worked Example

Consider a fully enclosed rotor that is 200 mm in diameter, running at 1500 r/min in air with a kinematic viscosity of 2e-5 m^2/s, with an annular gap of 1 mm. First, the critical speed is calculated from (15); this evaluates to $\Omega_{cr} = 82.2$ rad/s. Since the running speed of 1500 r/min is greater than this (157 rad/s), it is likely that there are vortices in the annulus.

The heat transfer can now be calculated. First, the quantity Ta^2/F_g^2 is calculated using (8) and (17). This equals to 6858. Since this is between 1700 and 10 000, (20) may be used to calculate the Nusselt number, giving $Nu = 3.27$. From the definition of the Nusselt number, the convective heat transfer coefficient is therefore equal to

$$h = \frac{Nu\,k}{D_h} = 47\ \mathrm{W/m^2 \cdot K} \tag{32}$$

where the hydraulic diameter $D_h = 2$ mm.

V. Disk Geometry Machines

Disk geometry machines have their air-gap magnetic field oriented in the axial direction. The most common type is the AFPM brushless machine, although other machines, including brushed dc and induction machines, are also possible. There are many different configurations, for example, rotor–stator, rotor–stator–rotor, stator–rotor–stator, and multiple disks, and

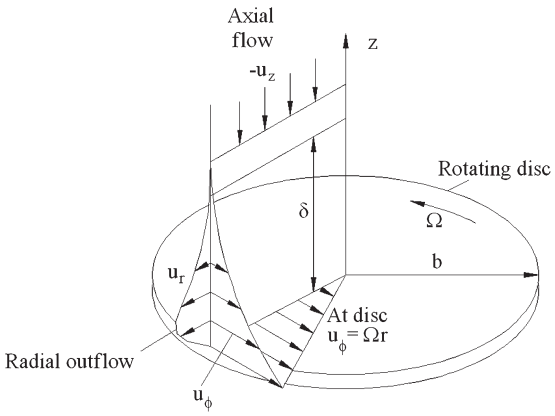

Fig. 3. Free rotor disk flow.

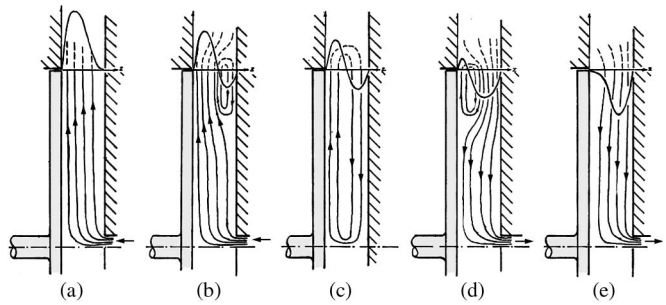

Fig. 4. Typical streamlines for laminar flow in small clearances with no case at the outer edge, from [29]. (a) Radial outflow with large pumping rate. (b) Radial outflow with smaller pumping rate (note separation bubble on stator). (c) No superposed flow. (d) Radial inflow with small pumping rate. (e) Radial inflow with large pumping rate.

both totally enclosed and throughflow-ventilated configurations are possible.

In a disk machine, the air-gap flow is pumped by a pressure difference caused by the rotation of the rotor(s). This makes disk machines fundamentally different to cylindrical machines, where any axial throughflow of air must be pumped by an externally imposed pressure difference. Heat typically from the stator is transferred to the fluid by forced convection at the stator surface. The configuration of the airflow path is crucial to the thermal performance.

A. Airflow in the Rotor–Stator Gap

A large body of analytical, numerical, and experimental research has been undertaken concerning airflow and heat transfer of a disk system. This is relevant to electrical machines, gas turbines, turbochargers, brake disks, and many other types of machine. Dorfman's book [24] concentrates on analytical solutions, with some experimental results. The book by Owen and Rogers [25] gives a comprehensive review of various analytical solutions and compares these with experimental data for free disk and rotor–stator systems with and without superposed flow, including heat transfer.

The simplest kind of rotating disk system is the "free disk," an infinite-radius rotating disk in a fluid. This was originally examined by von Kármán [26] who found a solution to the Navier–Stokes equations showing that the disk drags fluid from the rotor center to the outside edge, at the same time drawing fresh fluid inward axially as shown in Fig. 3. By assuming axisymmetry, he reduced the partial differential equations to a set of four coupled ordinary differential equations and solved the nondimensionalized equations for radial, tangential, and axial velocity components and pressure as a function of axial distance, by using approximate analytical (momentum-integral) methods, for both laminar flow and turbulent flow.

The same approach can be applied to a rotating fluid above a stationary surface where it is found that the opposite effect occurs, i.e., the fluid near the surface is slowed down and moves radially inward.

Batchelor [27] studied mathematically the flow between infinite coaxial disks using similar methods as those of von Kármán, proposing that, particularly at large Reynolds numbers, there would be an inviscid rotating fluid core between separate laminar or turbulent boundary layers located on the rotor and stator, respectively. The rotation speed of the core is approximately 40% of the rotor disk speed. This type of rotor–stator flow with core rotation is often called the "Batchelor flow." In the core itself, the fluid rotates with almost zero radial and axial velocity, and a radial pressure gradient balances the centrifugal force

$$\rho \frac{V_\theta^2}{r} = \frac{dp}{dr}. \tag{33}$$

In contrast, Stewartson [28] proposed alternatively that the tangential velocity drops away from the rotor surface to zero at the stator surface, with no core rotation. Until the 1980s, there was some controversy over which solution was correct. However, both authors based their calculations on infinite-diameter disks, and subsequently, it has been shown that, with finite-diameter disks, it is the condition at the boundary that determines whether the flow will tend toward a Batchelor pattern or a Stewartson pattern. Batchelor flow is usually observed in enclosed systems, but in systems which are open at the periphery and have radial throughflow, Stewartson flow may be seen.

Soo [29] analyzed the laminar flow over an enclosed rotor using approximate methods and suggests that, for rotor cooling, radial outflow is more effective than radial inflow. Fig. 4 shows a range of streamlines for the laminar case with open periphery and superposed in/outflow.

The smooth transition from Batchelor to Stewarston flow is illustrated by Poncet *et al.* [30], [31] who experimented with a rotor–stator system under three conditions: no superimposed throughflow, radial inflow, and radial outflow. They found that, when a radial inflow is superimposed, the flow remains a Batchelor type, but when a radial outflow is superposed, the flow becomes a Stewartson type, and the core rotation diminishes or disappears. The authors show that the transformation from Batchelor to Stewartson flow can be quantified directly.

For the case of an enclosed rotor–stator system with no throughflow, Daily and Nece [32] observed the following four distinct flow regimes depending on G and Re_θ:

1) merged laminar rotor and stator boundary layers, occurring for small values of G and Re_θ;

2) separate laminar boundary layers at larger values of G and small Re_θ;
3) merged turbulent boundary layers at smaller G values and larger Re_θ;
4) separate turbulent boundary layers at larger G and Re_θ values.

Regimes 2 and 4 correspond to a Batchelor-type flow with core rotation. The distinction between each regime is not sharp but occurs over a range of values of G and Re_θ.

In a disk-type electrical machine, a range of configurations is possible: The periphery may be fully enclosed, partially enclosed, or open but surrounded by a grill or mesh. There may be significant rotor-pumped radial throughflow. The flow may tend toward either a Batchelor or Stewartson pattern depending on the particular configuration, and the actual flow pattern may be a combination of both regimes.

In throughflow-ventilated disk machines, the size of the air inlet is very important in determining or limiting the amount of airflow through the system. Smaller air inlet sizes may restrict the air throughflow rate and therefore change the internal air-gap flow regime. Rotating air inlets exhibit a variety of different discharge coefficients that depend on the rotational speed and incidence angle [33].

B. Convective Heat Transfer

A variety of techniques has been applied to measure heat transfer in rotor–stator systems. Cobb and Saunders [34] applying the Reynolds analogy found that the turbulent rotor heat transfer correlation for a free disk could be derived accurately from rotor torque measurements. Owen [35] also applied the Reynolds analogy to a turbulent rotor–stator system and extended the concept to include frictional heating effects.

A recent direct measurement technique involves the numerical solution of the heat equation in a solid (either rotor or stator), using measured temperatures at various locations, for example, applied by Owen *et al.* [36] to measure both the rotor and stator heat transfer. Infrared thermography of rotor surface temperatures can be used with this method, as applied by Boutarfa and Harmand [37]. A thin layer of thermally insulating material (zirconia) is applied at the disk surface, and the temperature at the aluminium–zirconia junction is measured by embedded thermocouples. The heat flux through the rotor surface is found by solving the heat equation in the zirconia using a finite-difference method, applying the experimentally measured temperature boundary conditions. The surface heat flux is obtained from the temperature gradient at the surface.

A number of authors have derived and measured rotor heat transfer in the "free disk" case (see Fig. 3). The heat transfer correlations are usually given as a power law for the average Nusselt number as a function of the rotational Reynolds number

$$Nu = ARe_\theta^B. \tag{34}$$

In the case of the laminar flow ($Re_\theta < 1e5$), Dorfman's analytical correlation [24] has $A = 0.35$ and $B = 0.5$; Cobb and Saunders [34] give a similar correlation for an isothermal free rotor, with $A = 0.36$ and $B = 0.5$. Finally, Owen and Rogers [25] derive the values $A = 0.33$ and $B = 0.5$ by the numerical solution of the energy equation in the laminar free rotor case. Since, in all of these cases, $B = 0.5$, on substituting the definitions of the Nusselt number and the rotational Reynolds number into (34), the radius R cancels, and a direct relationship between the rotor speed and the convective heat transfer coefficient may be found

$$h \approx 0.35k\left(\frac{\Omega}{\nu}\right)^{0.5}. \tag{35}$$

A correlation for turbulent average Nusselt numbers (valid for $Re_\theta > 2.8e5$) for an isothermal free rotor is given by Owen *et al.* [36]

$$Nu = 0.0151Re_\theta^{0.8}. \tag{36}$$

TABLE II
ROTOR HEAT TRANSFER CORRELATIONS, BOUTARFA AND HARMAND [37]

G	Regime	Correlation
0.01	lam.	$Nu = 7.46Re_\theta^{0.32}$
0.02–0.06	lam.	$Nu = 0.5\left(1 + 5.47 \times 10^{-4}e^{112G}\right) Re_\theta^{0.5}$
0.01	turb.	$Nu = 0.044Re_\theta^{0.75}$
0.02–0.06	turb.	$Nu = 0.033\left(12.57e^{-33.18G}\right) Re_\theta^{0.6+25G^{12/7}}$

Boutarfa and Harmand [37] present experimentally measured correlations for rotor heat transfer in an open throughflow-ventilated rotor–stator system with varying gap ratios G, with no additional superposed airflow. Their correlations are presented in Table II with the four regimes corresponding to those given by Daily and Nece [32] previously. In all these cases, the reference temperature for the convective heat transfer coefficient is the fluid inlet temperature, which is usually ambient. As can be seen at $G = 0.01$, the rotor heat transfer is higher in the rotor–stator system compared with that in the free rotor, in both the laminar and turbulent regimes. At intermediate gap sizes $0.02 \leq G \leq 0.06$, the authors found that the rotor heat transfer drops to a minimum at $G \approx 0.02$, which is lower than the free rotor value, and then increases to the free rotor value at $G > 0.06$.

In the literature, stator heat transfer has received less attention than rotor heat transfer, although it is important in the design of disk-type machines since most of the heat is typically generated in the stator. Bunker *et al.* [38], with gas turbine internal air systems in mind, measured both rotor and stator heat transfer in a shrouded rotor–stator system with radial outflow using a central jet of air impinging on the rotor.

Recent work by Howey *et al.* [39], [40] measured radially resolved stator convective heat transfer in a generalized throughflow-ventilated disk machine, using a geometric mock-up of a machine. This comprised a heated stator surface adjacent to a 470-mm-diameter spinning aluminum rotor driven by a servomotor, with air admitted through an opening at the stator center and expelled at the periphery of the system. The gap size between the rotor and the stator was adjustable by inserting accurately machined spacers. Two types of rotor were tested: a flat rotor and also a rotor with protrusions designed to mimic the PMs of an AFPM machine. Gap ratios G from 0.01 to 0.05

TABLE III
AVERAGE STATOR HEAT TRANSFER TURBULENT CORRELATIONS

G	A	B
0.0106	0.0790	0.640
0.0127	0.0888	0.633
0.0170	0.0406	0.682
0.0212	0.0315	0.691
0.0297	0.0347	0.679
0.0467	0.0234	0.712

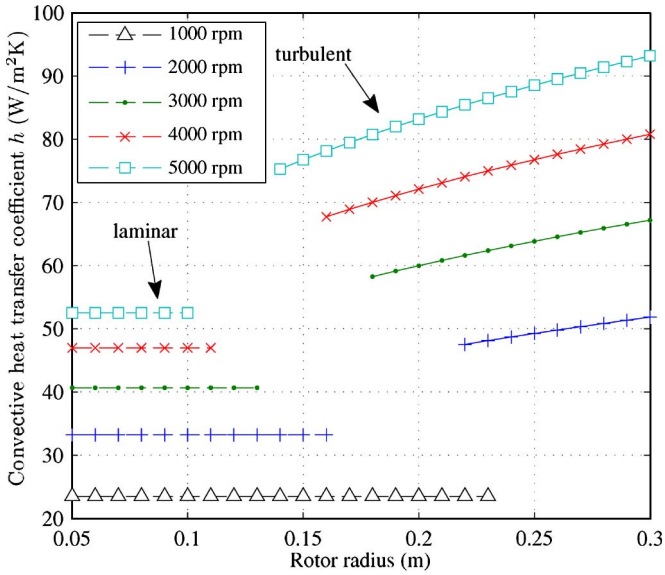

Fig. 5. Stator surface convective heat transfer coefficient of disk machine.

were tested, with rotational Reynolds numbers Re_θ from 3.7e4 to 1e6. The measurements were undertaken using a thin-film heating technique, enabling the direct measurement of the heat flux by the measurement of the electrical power into a heater array. It was found that average stator heat transfer results can be correlated according to the power law of (34), with constants A and B given in Table III. These are valid in the turbulent regime, with a range $Re_\theta \geq 5.19\text{e}5$. All values of B are similar, $B = 0.673 \pm 0.028$, but the values of A differ according to gap ratio G. In the laminar regime ($Re_\theta \leq 3\text{e}5$), it was found that the free *rotor* correlation can be reliably used at the stator to predict the heat transfer.

Fig. 5 shows how the convective heat transfer coefficient at the stator surface varies with the disk size and speed in the case of a disk-type machine with gap ratio $G = 0.01$, using (35) in the laminar case and the data from the first row of Table III in the turbulent case.

C. Worked Example

Consider a disk-type throughflow-cooled machine with a rotor that is 400 mm in diameter, running at 3000 r/min in air with a kinematic viscosity of 2e-5 m^2/s, with an axial rotor–stator gap of 4 mm. First, the rotational Reynolds number is calculated from (3) based on the speed and rotor outside radius: $Re_\theta = 6.3\text{e}5$, and it can be seen that the flow is turbulent both at the rotor and the stator surfaces. The gap ratio is $G = 0.01$; therefore, the appropriate rotor heat transfer correlation to use is $Nu = 0.044 Re_\theta^{0.75}$ from Table II, and this evaluates to Nu $= 982$. Therefore, $h = 126$ W/m$^2 \cdot$ K.

The stator heat transfer can also be calculated using (34) with values for A and B given in the first line of Table III, since $G \approx 0.01$. This gives $Nu_s = 406$, and therefore, $h_s = 60$ W/m$^2 \cdot$ K where, in both cases, the subscript s refers to the stator.

VI. CONCLUSION

The prediction of temperatures in electrical machines is vital to ensure that the designs deliver the required performance at the lowest cost. This paper has focused on air-gap convective heat transfer and has sought to give an overview of the work in this area, collecting and summarizing the key correlations and findings, including worked examples which are particularly relevant to smaller machines. Many correlations have arisen from work on turbomachinery but are equally applicable in electrical machine design and have not been presented previously in this context. It is hoped that designers can directly apply these correlations within thermal models to predict temperatures.

In all types of electrical machine, the air-gap convective heat transfer is not constant and is affected primarily by the rotating speed of the machine and the size of the rotor and air gap. In general, larger and faster machines have higher convective heat transfer coefficients in the air gap, while in smaller slower machines, the heat transfer coefficients are lower. Indeed, smaller fractional horsepower machines may struggle to achieve very high torque densities compared to larger machines. This is because, in a smaller machine, the temperature gradients in the flow are lower and because the flow is more likely to be laminar. Introducing externally pumped superposed airflow will increase the heat transfer in the gap, as will increasing the surface roughness of internal flow passages.

Although this paper has been divided into a section on cylindrical machines and a section on disk machines, both sections are relevant to the design of either types of machine since all machines have both "disk" faces and a "drum" section.

REFERENCES

[1] A. Boglietti, "Guest editorial," *IEEE Trans. Ind. Electron.*, vol. 55, no. 10, pp. 3498–3499, Oct. 2008.
[2] A. Boglietti, A. Cavagnino, D. Staton, M. Shanel, M. Mueller, and C. Mejuto, "Evolution and modern approaches for thermal analysis of electrical machines," *IEEE Trans. Ind. Electron.*, vol. 56, no. 3, pp. 871–882, Mar. 2009.
[3] D. Staton, A. Boglietti, and A. Cavagnino, "Solving the more difficult aspects of electric motor thermal analysis in small and medium size industrial induction motors," *IEEE Trans. Energy Convers.*, vol. 20, no. 3, pp. 620–628, Sep. 2005.
[4] A. Fitzgerald, C. Kingsley, and S. Umans, *Electrical Machinery*, 5th ed. New York: McGraw-Hill, 1990.
[5] J. Gieras, R. Wang, and M. Kamper, *Axial Flux Permanent Magnet Brushless Machines*, 2nd ed. New York: Springer-Verlag, 2008.
[6] C. Hernandez-Aramburo, T. Green, and S. Smith, "Assessment of power losses of an inverter-driven induction machine with its experimental validation," *IEEE Trans. Ind. Appl.*, vol. 39, no. 4, pp. 994–1004, Jul./Aug. 2003.
[7] Engineering Sciences Data Unit, *Flow in Rotating Components-Discs, Cylinders and Cavities, ESDU Data Sheet 07004*, 2007. IHS ESDU.
[8] P. Mellor, D. Roberts, and D. Turner, "Lumped parameter thermal model for electrical machines of TEFC design," *Proc. Inst. Elect. Eng. B—Elect. Power Appl.*, vol. 138, no. 5, pp. 205–218, Sep. 1991.

[9] E. Spooner and B. Chalmers, ""TORUS": A slotless, toroidal-stator permanent-magnet generator," *Proc. Inst. Elect. Eng. B—Elect. Power Appl.*, vol. 139, no. 6, pp. 497–506, Nov. 1992.
[10] D. Staton and A. Cavagnino, "Convection heat transfer and flow calculations suitable for electric machines thermal models," *IEEE Trans. Ind. Electron.*, vol. 55, no. 10, pp. 3509–3516, Oct. 2008.
[11] P. Childs and C. Long, "A review of forced convective heat transfer in stationary and rotating annuli," *Proc. Inst. Mech. Eng.C, Mech. Eng. Sci.*, vol. 210, no. C2, pp. 123–134, 1996.
[12] L. Rayleigh, "On the dynamics of revolving fluids," *Proc. R. Soc. Lond. A, Math. Phys. Sci.*, vol. 93, no. 648, pp. 148–154, Mar. 1917.
[13] G. Taylor, "Stability of a viscous liquid contained between two rotating cylinders," *Philos. Trans. Roy. Soc. London A, Math. Phys. Sci.*, vol. 223, pp. 289–343, Jan. 1923.
[14] I. Bjorklund and W. Kays, "Heat transfer between concentric rotating cylinders," *Trans. ASME, J. Heat Transf.*, vol. 81, pp. 175–186, 1959.
[15] K. Becker and J. Kaye, "Measurements of diabatic flow in an annulus with an inner rotating cylinder," *Trans. ASME, J. Heat Transf.*, vol. 84, pp. 97–105, 1962.
[16] K. Becker and J. Kaye, "The influence of a radial temperature gradient on the instability of fluid flow in an annulus with an inner cylinder rotating," *Trans. ASME, J. Heat Transf.*, vol. 84, pp. 106–110, 1962.
[17] J. Kaye and E. Elgar, "Modes of adiabatic and diabatic flow in an annulus with inner rotating cylinder," *Trans. ASME*, vol. 80, pp. 753–765, 1958.
[18] D. Simmers and J. Coney, "A Reynolds analogy solution for the heat transfer characteristics of combined Taylor vortex and axial flows," *Int. J. Heat Mass Transf.*, vol. 22, no. 5, pp. 679–689, May 1979.
[19] C. Gazley, "Heat transfer characteristics of the rotational and axial flow between concentric cylinders," *Trans. ASME*, vol. 80, pp. 79–90, 1958.
[20] S. Kosterin and Y. Finatev, "Heat transfer in turbulent airflow the annular space between rotating coaxial cylinders," *Inzh.-Fiz. Zh.*, vol. 8, pp. 3–9, 1962, (in Russian).
[21] T. Kuzay and C. Scott, "Turbulent heat transfer studies in annulus with inner cylinder rotation," *Trans. ASME, J. Heat Transf.*, vol. 99, pp. 12–19, 1977.
[22] P. Childs, A. Turner, C. Vaughan, D. Rayner, and F. Bayley, "Heat transfer to a rotating drum in an annulus with a stator blade row and axial throughflow," presented at the 37th ASME Int. Gas Turbine Aeroengine Congr. Expo., Cologne, Germany, 1992, ASME Paper 92-GT-249.
[23] P. Childs and A. Turner, "Heat transfer on the surface on the surface of a cylinder rotating in an annulus at high axial and rotational Reynolds number," in *Proc. 10th Int. Heat Transf. Conf.*, Brighton, U.K., 1994, vol. 3, pp. 13–18.
[24] L. Dorfman, *Hydrodynamic Resistance and the Heat Loss of Rotating Solids*. Edinburgh, U.K.: Oliver & Boyd, 1963.
[25] J. Owen and R. Rogers, *Flow and Heat Transfer in Rotating-Disc Systems, Vol. 1: Rotor–Stator Systems*, 1st ed. Taunton, U.K.: Res. Stud. Press, 1989.
[26] T. von Kármán, "Über laminare und turbulente Reibung," *Z. Angew. Math. Mech.*, vol. 1, no. 4, pp. 233–235, 1921.
[27] G. Batchelor, "Note on a class of solutions of the Navier–Stokes equations representing steady rotationally-symmetric flow," *Q. J. Mech. Appl. Math.*, vol. 4, no. 1, pp. 29–41, 1951.
[28] K. Stewartson, "On the flow between two rotating coaxial discs," *Math. Proc. Camb. Philos. Soc.*, vol. 49, no. 2, pp. 333–341, 1953.
[29] S. Soo, "Laminar flow over an enclosed rotating disk," *Trans. ASME*, vol. 80, no. 2, pp. 287–296, 1958.
[30] S. Poncet, M. Chauve, and R. Schiestel, "Batchelor versus Stewartson flow structures in a rotor–stator cavity with throughflow," *Phys. Fluids*, vol. 17, no. 7, p. 075 110, Jul. 2005.
[31] S. Poncet, R. Schiestel, and M. Chauve, "Centrifugal flow in a rotor–stator cavity," *Trans. ASME, J. Fluids Eng.*, vol. 127, pp. 787–794, 2005.
[32] J. Daily and R. Nece, "Chamber dimension effects on induced flow and frictional resistance of enclosed rotating disks," *Trans. ASME, J. Basic Eng.*, vol. 82, no. 1, pp. 217–232, 1960.
[33] A. Idris, K. Pullen, and D. Barnes, "An investigation into the flow within inclined rotating orifices and the influence of incidence angle on the discharge coefficient," *Proc. Inst. Mech. Eng. A, J. Power Energy*, vol. 218, no. 1, pp. 55–68, 2004.
[34] E. Cobb and O. Saunders, "Heat transfer from a rotating disk," *Proc. R. Soc. Lond. A, Math. Phys. Sci.*, vol. 236, no. 1206, pp. 343–351, Aug. 1956.
[35] J. Owen, "The Reynolds analogy applied to flow between a rotating and a stationary disc," *Int. J. Heat Mass Transf.*, vol. 14, no. 3, pp. 451–460, Mar. 1971.
[36] J. Owen, C. Haynes, and F. Bayley, "Heat transfer from an air-cooled rotating disk," *Proc. R. Soc. Lond. A, Math. Phys. Sci.*, vol. 336, no. 1607, pp. 453–473, Feb. 1974.
[37] R. Boutarfa and S. Harmand, "Local convective heat transfer for laminar and turbulent flow in a rotor–stator system," *Exp. Fluids*, vol. 38, no. 2, pp. 209–221, Feb. 2005.
[38] R. Bunker, D. Metzger, and S. Wittig, "Local heat transfer in turbine disk cavities: Part I, Rotor and stator cooling with hub injection of coolant," *Trans. ASME, J. Turbomach.*, vol. 114, no. 1, pp. 211–220, Jan. 1992.
[39] D. Howey, A. Holmes, and K. Pullen, "Radially resolved measurement of stator heat transfer in a rotor–stator disc system," *Int. J. Heat Mass Transf.*, vol. 53, no. 1–3, pp. 491–501, Jan. 2010.
[40] D. Howey, A. Holmes, and K. Pullen, "Prediction and measurement of heat transfer in air-cooled disc-type electrical machines," in *Proc. IET, PEMD Conf.*, Brighton, U.K., Apr. 19–21, 2010, pp. 1–6.

David A. Howey (M'11) received the M.Eng. degree in electrical and information sciences from Cambridge University, Cambridge, U.K., in 2002, and the Ph.D. degree from Imperial College London, London, U.K., in 2010, investigating air-gap convective heat transfer in disk-type electrical machines.

He is a Research Associate with the Mechanical Engineering Department, Imperial College London. His current research interests include the thermal analysis of electrical machines and batteries, centimeter-scale wind turbines for energy harvesting, and electrically assisted turbochargers for large off-road diesel engine vehicles.

Peter R. N. Childs received his B.Sc. and D.Phil. degrees from University of Sussex, Brighton, U.K.

He is the Professorial Lead in Engineering Design with Imperial College London, London, U.K., where he leads the Design Engineering group and is the Joint Course Director for the Innovation Design Engineering degree at the Royal College of Art and Imperial. His general interests include creativity and the use of creativity tools, mechanical design, rotating flow, heat transfer, and sustainable energy. He was formerly the Director of InQbate, a Centre of Excellence in Teaching and Learning in Creativity, and director of the Rolls-Royce supported University Technology Centre for Aero-Thermal Systems at the University of Sussex. He has recently published a book on rotating flow.

Andrew S. Holmes (M'03) received the B.A. degree in natural sciences from Cambridge University, Cambridge, U.K., in 1987, and the Ph.D. degree in electrical engineering from Imperial College London, London, U.K., in 1992.

He is currently Professor of microelectromechanical systems (MEMS) with the Optical and Semiconductor Devices Group, Department of Electrical and Electronic Engineering, Imperial College London. His main research interests include micropower generation and conversion, MEMS devices for microwave applications, and laser processing for MEMS manufacture.